



## GROWTH OF INTERNAL DELAMINATIONS UNDER CYCLIC COMPRESSION IN COMPOSITE PLATES

G. A. KARDOMATEAS, A. A. PELEGRI and B. MALIK

School of Aerospace Engineering, Georgia Institute of Technology,  
Atlanta, Georgia 30332-0150, U.S.A.

(Received 4 May 1994; in revised form 28 January 1995)

### ABSTRACT

The growth of internal delaminations in composite plates subjected to cyclic compression is investigated. Due to the compressive loading, these structures undergo repeated buckling-unloading of the delaminated layer with a resulting reduction of the interlayer resistance. An important characteristic of the problem is that the state of stress near the delamination tip is of mixed mode, I and II. Equations describing the growth of the delaminations under cyclic loads are obtained on the basis of a combined delamination buckling-post-buckling and fracture mechanics model. The latter is based on a mode-dependent critical fracture energy concept and is expressed in terms of the spread in the energy release rate in the pre- and post-buckling state. It is shown that such a model allows for the accumulation of microdamage at the delamination front. The growth laws developed in this manner are integrated numerically, in order to produce the delamination growth vs number of cycles curves. Furthermore, the investigation includes the possibility of unstable delamination growth. The study does not impose any restrictive assumptions regarding the delamination thickness and plate length (as opposed to the usual thin film assumptions). The results show that for a given value of delamination thickness  $h$ , the fatigue delamination growth is strongly affected by the relative location of the delamination through the plate thickness  $T$ , the fatigue growth being slower for a smaller value of  $h/T$  (delaminations located closer to the surface). These theoretical predictions are confirmed by experimental results that are obtained for the growth of delaminations in graphite-epoxy unidirectional specimens under cyclic constant amplitude compressive loading. The test data, which were obtained for several different locations of the delamination through the thickness (hence different degrees of mode mixity), and different applied maximum compressive displacement, seem to be well-correlated with the theory.

### 1. INTRODUCTION

One of the most serious problems associated with laminated composites is the formation of an internal delaminated zone, i.e. two adjacent layers are partially debonded at their interface. This occurs most commonly as a consequence of low-velocity impact, but it may also be pre-existing due to manufacturing imperfections. There may be other reasons that cause delaminations such as vibrations excited by the propulsion systems.

Under compression loading, the delaminated layer may buckle. This local instability does not necessarily imply the ultimate load, and usually the laminate is capable of carrying on in the post-buckling phase under higher loading. However, the buckling-induced stresses at the tip of the delamination may cause growth of the interlayer crack and eventual complete separation of the layer. Besides strength and stiffness,

delaminations can influence other performance characteristics, such as the energy absorption capacity of composite beam systems (Kardomateas and Schmueser, 1988).

The prospect of local delamination buckling, and especially the possibility of growth, detracts from the high potential of composites and needs to be well-understood so that composites can be safely used in compressive load bearing applications with confidence. This is one of the compressive failure modes, and other frequently observed modes include microcracking and kinking. Accordingly, this subject of delamination buckling has become the topic of numerous publications over the last decade. However, although the bifurcation point in the context of a delaminated beam/plate has been investigated extensively in both one- and two-dimensional treatments (e.g. Chai *et al.*, 1981; Evans and Hutchinson, 1984; Chai and Babcock, 1985; Simitzes *et al.*, 1985; Wang *et al.*, 1985), the post-buckling behavior has been studied to a lesser extent. Furthermore, most studies in the literature have addressed the theoretical aspects, while the few experimental ones on delamination buckling have focused on static (monotonic) loading (Kardomateas, 1990). Regarding the fatigue growth of delaminations, Russell and Street (1987, 1988) have performed experiments on graphite-epoxy specimens under pure Mode I or pure Mode II loading.

The growth behavior of delaminations has been generally studied by using the Griffith-Irwin concept of critical fracture energy. A fundamental question is the extent to which delamination growth may be adequately represented through simply a mode-independent energy release rate criterion rather than employing a more complicated criterion that includes the mode mixity (ratio of Mode II to Mode I). Recent experimental studies on several composites have clearly shown that a mode-independent approach would be inadequate (O'Brien, 1990; Chai, 1992).

The practical significance of the problem under consideration is underlined by the fact that the more or less standard design for aircraft structures consists of thin skin, possibly strengthened by longitudinal stiffeners or lateral frames. Aerodynamic loading induces lateral bending, with one side being subjected to compression. As a consequence, delaminations on the compressed part of the structure can undergo local buckling, which effectively induces stress concentrations at the delamination front. On load removal, the delaminated layer returns to its undeflected position (unless the deflections are very large and the material has some ductility, which would cause permanent plastic deformations). Cyclical loading of compressed panels with delaminations (and hence repeated delamination buckling) causes a reduction of interlayer resistance as a result of damage accumulation at the tip. Therefore, delaminations that would not propagate under static loading, may grow and cause failure after a sufficient number of compression cycles.

The problem of determining the post-buckling deflections of a thin debonded layer when a plate element is subjected to cyclic compression is geometrically nonlinear, and the explicit presence of additional parameters with the dimension of the length (e.g. the thickness of the separated layer) makes it a nontraditional problem of fracture mechanics. Additional complications are introduced by the circumstance that the process of separated-layer growth may be accompanied by the phenomenon of elastic instability of the entire structural element.

Chai *et al.* (1981) presented a one-dimensional model by assuming essentially a delamination in an infinitely thick plate. In this model, which has also been called the

"thin film" model, the unbuckled (base) plate is assumed to be subject to a uniform compressive strain. In the general case, the finite plate length and thickness is expected to influence the bifurcation point and post-critical behavior of the delamination and subsequently its growth characteristics. An additional influence may also arise from the end fixity conditions of the base plate. To this extent, Simitse *et al.* (1985) studied the critical load for a delamination of arbitrary thickness and size in a finite plate; their results showed a range of critical load vs thin film load ratios, depending on delamination and base plate dimensions, as well as base plate end fixity (simply-supported vs clamped). Concerning the post-critical behavior of delaminations of arbitrary size, Kardomateas (1989) provided a formulation for studying the post-buckling behavior by using elastica theory for representing the deflections of the buckled layer; this work resulted in a system of nonlinear equations rather than closed form expressions. The post-critical behavior was also studied by Sheinman and Adan (1987) through a high-order kinematic model, with the nonlinear differential equations solved by Newton's method and a special finite-difference scheme. A more complete list of contributions on the subject including some early papers can be found in Storåkers (1989).

In a recent paper, Kardomateas (1993) studied the initial post-buckling behavior of general delaminated composites (i.e. with no restrictive assumptions on the delamination dimensions) by using a perturbation procedure based on an asymptotic expansion of the load and deformation quantities in terms of the distortion parameter of the delaminated layer, the latter being considered a compressive elastica. The analysis lead to closed form solutions for the load vs applied compressive displacement and the near tip resultant moments and forces. An extended analysis considered the effects of the end conditions, i.e. clamped-clamped or simply-supported (Kardomateas and Pelegri, 1995). In these studies, the bimaterial interface crack solutions for the mode mixity and the energy release rate in terms of the resultant moments and forces, as derived by Suo and Hutchinson (1990) were subsequently employed. These relations are actually simplified because the material is assumed homogeneous. This post-buckling solution was used in a subsequent study by Kardomateas and Pelegri (1994) to study the stability of growth of internal delaminations as well as some other important characteristics of the growth process. A primary objective of that work was to define the combinations of delamination length and applied strain that lead to unstable growth; this would practically cause either contained "jump" growth or catastrophic (complete) growth of the delamination. A major conclusion of the Kardomateas and Pelegri (1994) study was that delamination growth is more likely to be stable than would be predicted by the thin film model.

In the present paper, the fatigue growth of delaminations under constant amplitude cyclic compression is studied. Some results are extracted from the earlier post-buckling solution of Kardomateas (1993) and they are used in conjunction with a proposed mixed-mode cyclic growth law that essentially accounts for the accumulation of microdamage at the delamination front during the loading-unloading cycles. An experimental program is undertaken on graphite-epoxy, with delaminations located at different locations through the specimen thickness (hence at different prevailing mode mixities) and with different applied external displacements. The configuration involves the simple one-dimensional through-the-width delaminations and can be

used as a benchmark configuration for studying the fatigue behavior before further extensions to the more complex two-dimensional delaminations are attempted.

The growth law is a function of the spread in the energy release rate in the pre- and post-buckled states and the maximum value of the energy release rate in the cycle, both normalized with the mode-dependent interface fractures toughness. The exponent and the constant of the growth law are also taken to be mode dependent. The delamination growth vs number of cycles curves are produced by integrating numerically the growth laws developed in this manner. The predictive capability of the procedure is illustrated by correlating the data from the experiments.

## 2. CHARACTERISTICS OF THE CYCLICLY COMPRESSED DELAMINATION

### 2.1. Mode mixity and energy release rate at the initial post-buckling phase

The major characteristic of delamination growth is the fact that the fracture path is constrained irrespective of the application of the globally-applied loads, hence growth is inherently mixed mode. In the present compressive loading problem, the initial post-buckling deformations of the delaminated system define the conditions for determining the state of stress at the delamination tip. Referring to Fig. 1, consider a plate of half-length  $L$  (and unit width) with a through-the-width delamination of half-length  $l$ , symmetrically located. The delamination is at an arbitrary position through the thickness  $T$ . Over the delaminated region, the laminate consists of the part above the delamination, of thickness  $h$ , referred to as the "delaminated" part,

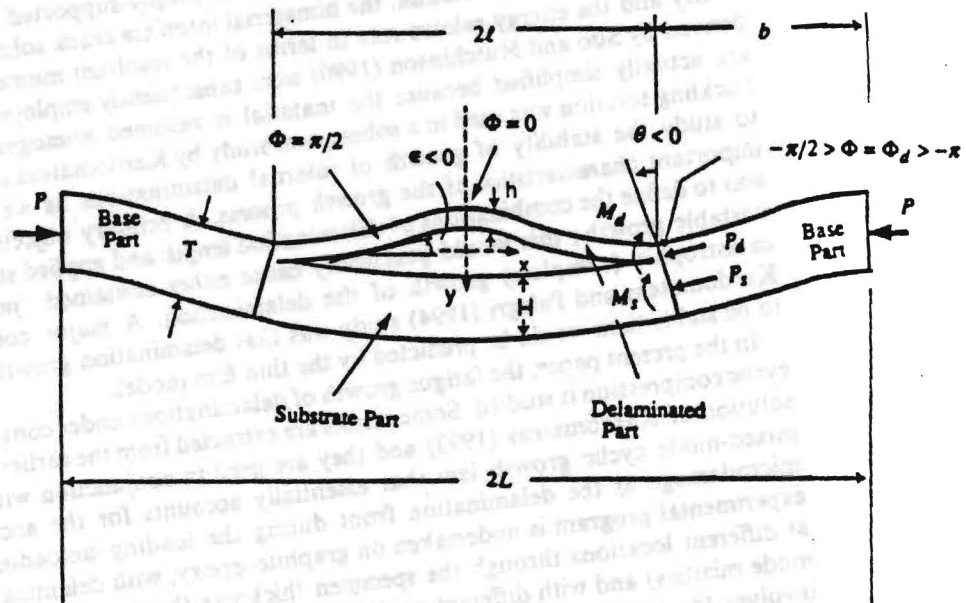


Fig. 1. A one-dimensional delamination configuration under compression.

and the part below the delamination, of thickness  $H = T - h$ , referred to as the "substrate" part. The remaining, intact laminate, of thickness  $T$  and length  $b = L - l$ , is referred to as the "base" plate. Accordingly, the subscript  $i = d, s, b$  refers to the delaminated part, the substrate or the base plate, respectively.

A closed form solution for the initial post-buckling behavior in the general case (arbitrary delamination thickness or plate length) has recently been derived by Kardomateas (1993). The latter is based on considering the buckled configuration of the delaminated layer as part of an inflectional elastica with end amplitude  $\Phi_d$  and distortion parameter  $\varepsilon$ .

This initial post-buckling solution is used in conjunction with the interface crack solutions summarized by Hutchinson and Suo (1992). Specifically, for the plane-strain interface crack shown in Fig. 1, the energy release rate  $G$  is:

$$G = \frac{1}{2E_L} \left[ \frac{P^{*2}}{Ah} + \frac{M^{*2}}{Ih^3} + 2 \frac{P^* M^*}{\sqrt{Ah^2}} \sin \gamma \right], \quad (1)$$

where  $\mu$  is the shear modulus and  $P^*$  and  $M^*$  are linear combinations of the loads at the common section (from the post-buckling solution). These quantities, along with the other constants in (1) are defined in Kardomateas (1993).

The preceding formula does not separate the opening and shearing components. Instead, the following two expressions give the Mode I and Mode II stress intensity factors:

$$K_I = \frac{1}{\sqrt{2}} \left[ \frac{P^*}{\sqrt{Ah}} \cos \omega + \frac{M^*}{\sqrt{Ih^3}} \sin(\omega + \gamma) \right], \quad (2a)$$

$$K_{II} = \frac{1}{\sqrt{2}} \left[ \frac{P^*}{\sqrt{Ah}} \sin \omega - \frac{M^*}{\sqrt{Ih^3}} \cos(\omega + \gamma) \right]. \quad (2b)$$

The mode mixity is defined by

$$\psi = \tan^{-1}(K_{II}/K_I). \quad (3)$$

Substituting the asymptotic expressions for the forces and moments from the post-buckling solution, gives the energy release rate and the Mode I and II stress intensity factors in the form:

$$G = \varepsilon^2 G^{(2)} + \varepsilon^3 G^{(3)} + \dots, \quad (4a)$$

$$K_{I,II} = \varepsilon K_{I,II}^{(1)} + \varepsilon^2 K_{I,II}^{(2)} + \dots \quad (4b)$$

The other quantity that is needed to correlate with the experiments is the applied strain,  $\varepsilon_0$ , which is the external "loading" quantity. This is given in a similar fashion, as follows:

$$\varepsilon_0 = \varepsilon_0^{(0)} + \varepsilon_0^{(1)} \varepsilon + \varepsilon_0^{(2)} \varepsilon^2, \quad (5)$$

where  $\varepsilon_0^{(j)}$ ,  $j = 0, 1, 2$  are again given in Kardomateas (1993).

Under certain conditions delamination growth may be unstable. Kardomateas and Pelegri (1994) examined the conditions for unstable delamination growth. In order

to assess the stability of growth, the construction of a  $G-l$  curve (for a constant applied compression  $\varepsilon_0 = E_0$ ) or a  $E_0-l$  curve (for a specified  $G = \Gamma_0$ ) is needed. Let us discuss the family curves of the energy release rate, as a function of delamination length,  $G(l)$ , for different values of applied strain  $\varepsilon_0$ . For a specified  $\varepsilon_0 = E_0$ , the corresponding  $\varepsilon$  is determined from the minimum (negative) root of the equation:

$$E_0 = \varepsilon_0^{(0)}(l) + \varepsilon_0^{(1)}(l)\varepsilon + \varepsilon_0^{(2)}(l)\varepsilon^2. \quad (6)$$

Then, the corresponding energy release rate is

$$G(l) = G^{(2)}(l)\varepsilon^2 + G^{(3)}(l)\varepsilon^3. \quad (7)$$

The delamination growth is stable if the  $G-l$  curve has a negative slope, in which case the  $\varepsilon_0-l$  curve has a positive slope, and it is unstable otherwise (Kardomateas and Pelegri, 1994). Hence, at the applied compression  $E_0$ , a "transition" delamination length is defined,  $l_{tr}$ , at which a transition occurs from unstable-to-stable delamination growth. This point is the peak (or zero slope) point on the curves of energy release rate vs delamination length.

The formulation presented hereby is a closed form solution, hence results can be produced for a variety of configurations with minimum effort. Alternative numerical (finite element) strategies have been pursued to investigate buckling-induced delamination growth such as by Nilsson and Storåkers (1992). These detailed finite element studies can provide answers to some of the more complex questions, such as the effect of a general anisotropy (rather than pure orthotropy), and possible contact effects that may arise after large amounts of growth, and which cannot be handled by the present formulation. Moreover, they can be used to solve the more complex two-dimensional configurations. A numerical study such as by Nilsson and Storåkers (1992) could also provide improved estimates for the delamination tip stress intensity factors by relaxing the restrictive assumptions in the interface crack solutions of Hutchinson and Suo (1992), which are asymptotic ones for cracks of infinite length. However, employing detailed finite element procedures would make for a very involved task in studying fatigue delamination growth, since cyclic growth involves a continuous change in delamination length and hence requires a very large number of different geometric configurations and meshes. For the simple, one-dimensional delamination that is considered in this paper, the closed form solution of Kardomateas (1993) provides an adequate means of capturing the effects of relative delamination thickness and delamination length, hence allowing to focus on the mechanics of cyclic growth, which is considered next.

## 2.2. Mode-dependent cyclic growth law

Several investigators have analyzed the strain energy release rate  $G$ , with respect to predicting edge or internal delamination growth. To this extent, a Griffith-type fracture criterion is employed and it is assumed that whether further delamination occurs depends on the magnitude of the fracture energy, defined as the energy required to produce a unit of new delamination. In mixed mode linear elastic fracture mechanics configurations, this quantity is uniquely expressed in terms of the Mode I and II stress intensity factors,  $K_I$  and  $K_{II}$ , respectively (e.g. Hellan, 1984).

During the initial post-buckling phase, the mode mixity changes with applied strain, and depends on the relative delamination thickness  $h/T$ . For example, the study by Kardomateas (1993) has shown that a higher Mode I component is present with delaminations further away from the surface. The mode mixity also changes as the delamination grows. Results that follow in the next section show clearly an increased Mode II component as the delamination propagates under a constant applied compressive strain.

For a cyclic loading that causes a variation of the strain energy release rate from  $G_{\min}$  to  $G_{\max}$ , the stresses near the tip of the delamination are completely described by  $G_{\max}$ , the load ratio  $\alpha = G_{\min}/G_{\max}$ , which expresses the ratio of minimum to maximum loading, and the mixity parameter,  $\psi = \tan^{-1}(K_{II}/K_I)$  that expresses the relative amounts of Mode I (opening) and Mode II (shearing) components. This is because these three parameters describe both the intensity and variation of the stress field near the delamination tip due to the loading and geometry configuration.

During a cycle of loading the stresses and strains near the tip of a delamination are completely specified by  $G_{\max}$ ,  $\alpha$  and  $\psi$ , so we can reasonably assume that any phenomenon occurring in this region is in general controlled by these parameters. The amount of crack extension per cycle of loading is just such a phenomenon, or, in functional form:

$$\frac{da}{dN} = f(G_{\max}, \alpha, \psi). \quad (8)$$

The mode dependence of the delamination growth process is not yet fully understood and is a subject of intense current research. In a recent paper, Chai (1992) conducted an experimental evaluation of mixed-mode fracture in adhesive bonds in order to elucidate the effect of the mode of loading on the interlaminar fracture toughness. The mixed-mode fracture behavior was characterized by essentially two bond thickness regimes. In the first, which is limited to a few micrometers, mode interaction occurred promptly upon the application of any combination of loads. In the second regime (thickness of more than about  $5 \mu\text{m}$ ), mode interaction occurred only when the shearing component of the energy release rate exceeded a certain value. In the case of the ductile BP-907 adhesive, that value was approximately 55% of the pure Mode II toughness,  $G_{II}^*$ . Below this value of  $G_{II}$ , the fracture toughness was that for pure Mode I,  $G_I^*$ . Test methods for determining the Mode I,  $G_I^*$ , and Mode II,  $G_{II}^*$ , fracture toughness for different composite systems as well as the resulting fracture toughness values have been reviewed by Sela and Ishai (1989). Of these, the most widely used are the double cantilever beam (DCB) test for  $G_I^*$  and the end notched flexural (ENF) test for  $G_{II}^*$ .

Because the interlaminar resin-rich layer in laminated composites is typically several micrometers thick, one would expect the composites mixed-mode interlaminar fracture to be characterized by some degree of prompt interaction between the modes.

In a related study on glass-epoxy, Liechti and Chai (1992) measured the toughness of the glass-epoxy interface over a wide range of mode mixes and found a toughening effect associated with increasing in-plane shear components. Optical interference measurements of the normal crack opening displacement that were made near the

crack front revealed large variations in plastic zone size with mode mix. The plastic zone sizes followed the same trends that the toughness exhibited with mode mix. Although all yielding was small scale in nature, there were large increases in size as the shear component increased.

Based on these observations, let us now assume that the toughness  $\Gamma_0$  depends on the mode mixity  $\psi$ , and in fact  $\Gamma_0(\psi)$  increases with increasing  $|\psi|$  (increasing mode II component). A simple, one parameter family of mixed-mode adjusted fracture criteria has been described by Hutchinson and Suo (1992):

$$\Gamma_0(\psi) = G_I^c [1 + (\lambda - 1) \sin^2 \psi]^{-1}. \quad (9)$$

The parameter  $\lambda$  adjusts the influence of the Mode II contribution in the criterion and should be determined experimentally by obtaining mode-interaction curves as in Chai (1992). Since for Mode I,  $\psi = 0$ ,  $\Gamma_0 = G_I^c$  and at Mode II,  $\psi = \pm 90^\circ$ ,  $\Gamma_0 = G_{II}^c$ , the expression (9) indicates that we may set

$$\lambda = G_I^c / G_{II}^c. \quad (9a)$$

where  $G_I^c, G_{II}^c$  are the values of the pure Mode I and pure Mode II toughness, respectively. For graphite-epoxy, a value of  $\lambda = 0.30$  is typical. The limit  $\lambda = 1$  is the case of the classical mode-independent toughness, i.e.  $\Gamma_0 = G_I^c$  for all mode combinations.

Other phenomenological criteria have been proposed to characterize mixed-mode toughness data for interlaminar fracture such as in Kinloch (1987). One other alternative phenomenological criterion is  $\Gamma_0(\psi) = G_I^c [1 + (1 - \lambda) \tan^2 \psi]$ . The latter models the toughness as unbounded as  $\psi \rightarrow 90^\circ$  for all  $\lambda < 1$ , unlike (9), for which the fracture toughness levels off as  $\psi \rightarrow 90^\circ$  (Mode II). As was discussed by Hutchinson and Suo (1992), while this feature should not be taken literally, it did emerge in the simple model of mixed-mode interface toughness due to asperity contact of Evans and Hutchinson (1989). In the present treatment, (9) is adopted to represent the mode-dependent interface toughness.

Returning now to the delamination growth in the initial post-buckling phase during cyclic compression, the effects of mode-dependent toughness on the growth characteristics can be accounted for by defining:

$$\tilde{G} = \frac{G}{\Gamma_0(\psi)} = \tilde{G}(\epsilon_0, \psi). \quad (10)$$

Then  $\tilde{G}$  can be regarded as a mode-adjusted crack driving force in the sense that the criterion for crack advance is  $G/\Gamma_0(\psi) = 1$ .

For the general case of arbitrary delamination and plate dimensions subjected to cyclic compression from the unloaded position to a maximum compressive strain  $\epsilon_{\max}$ , the post-buckling solution by Kardomateas (1993) can be used to derive the mode mixity  $\psi$  in a closed form expression. To assess whether slow fatigue growth would occur rather than unstable jump growth, the curve of the energy release rate at the maximum strain  $\tilde{G}_{\max} = G_{\max}/\Gamma_0(\psi)$ , as a function of delamination length for the specified applied strain  $\epsilon_0 = \epsilon_{\max}$  is plotted. For this specified  $\epsilon_0 = \epsilon_{\max}$ , the corresponding  $\epsilon$  is again determined from the minimum (negative) root of (6) and the corresponding energy release rate  $G$  is again found from (7). The mode mixity  $\psi$  is found from

$$\psi = \tan^{-1} \frac{\varepsilon K_{II}^{(1)} + \varepsilon^2 K_{II}^{(2)}}{\varepsilon K_I^{(1)} + \varepsilon^2 K_I^{(2)}} \quad (11)$$

For the experiments considered here, the minimum load is near zero, therefore  $\alpha = 0$ . The experimental data should then form a single curve on a plot of  $da/dN$  vs  $G_{\max}$  for different thicknesses, widths and lengths, testing frequencies and maximum loads. However, if partial unloading occurs, then both maximum and minimum loads correspond to different post-buckling states, and  $G_{\min} \neq 0$ .

Assuming that slow growth takes place, based on the above arguments, the following general power law relation is postulated for the cyclic delamination growth:

$$\frac{da}{dN} = C(\psi) \frac{(\Delta \bar{G})^{m(\psi)}}{1 - \bar{G}_{\max}} \quad (12)$$

$\Delta \bar{G}$  is the range in the energy release rate (normalized with the mode-dependent fracture toughness),  $\Delta \bar{G} = \bar{G}_{\max} - \bar{G}_{\min}$ . The denominator was introduced to model the very short life (typically less than  $10^3$  cycles), near the fracture toughness region. Hence, as  $\bar{G}_{\max}$  approaches unity, which means that  $G_{\max}$  approaches  $\Gamma_0(\psi)$  (the fracture toughness), a sharp upturn in the  $da/dN$  vs  $\Delta \bar{G}$  curve is predicted by (12). In this sense, (12) has a structure similar to Forman's (1967) Mode I equation for fatigue crack growth. However, outside this region, the denominator has a negligible influence. The well-known Paris fatigue law also has a similar power law structure but uses the stress intensity factor  $\Delta K$  for a single pure mode.

The mode dependence of the  $C$  and  $m$  constants in the growth law has been demonstrated experimentally by Russell and Street (1987, 1988). In essence, the growth rate,  $da/dN$ , under pure Mode I was less than expected on the basis of a mode-independent assumption for  $C$  and  $m$ , partly because of fiber bridging which occurs in Mode I. Although a slightly different growth law was used, for AS4/3501-6 graphite-epoxy, these constants were  $C_I = 0.0325$  and  $m_I = 5.8$  and for pure Mode II,  $C_{II} = 0.285$  and  $m_{II} = 9.4$ .

Of the two parameters, the most important is the exponent,  $m$ . Now, following the format of (9) for the mode dependence of the fracture toughness, we can set

$$m(\psi) = m_I [1 + (\mu - 1) \sin^2 \psi], \quad (13)$$

where, again since at pure Mode I,  $\psi = 0$ ,  $m = m_I$  and at pure Mode II,  $\psi = \pm 90^\circ$ ,  $m = m_{II}$ , the expression (13) suggests that  $\mu$  is defined as the ratio of the exponents  $m$  at Modes II and I, respectively:

$$\mu = m_{II}/m_I. \quad (13a)$$

In general,  $\mu$  is less than one. For graphite-epoxy, our experiments determined a value of  $\mu = 0.50$ , which agrees with the value determined by Russell and Street (1987, 1988) by conducting pure Mode I and II tests in double cantilever beam and end-delaminated flexure specimens.

In a similar fashion, concerning the first growth law constant,  $C(\psi)$ , we can set, following (9),

$$C(\psi) = C_I [1 + (\kappa - 1) \sin^2 \psi], \quad (14)$$

where,  $C_I$  is the constant  $C$  at pure Mode I, and, again  $\kappa$  is defined as the ratio of the constant  $C$  at Modes II and I, respectively:

$$\kappa = C_{II}/C_I. \quad (14a)$$

In general,  $\kappa$  is greater than one. For graphite epoxy, our experiments indicated a value of  $\kappa = 10$ , which again is close to the value determined by Russell and Street (1987, 1988). These constants can be determined independently. Specifically, Mode II fatigue testing can be carried out by using end-delaminated flexure specimens as in Russell and Street (1987). Pure Mode I fatigue testing can be carried out by using a uniform width and thickness double cantilever beam specimen (Russell and Street, 1988). These tests would allow determining  $C_{I,II}$ ,  $m_{I,II}$  and hence  $\mu$  and  $\kappa$ . The same tests can be performed statically to allow measuring  $G_I^c$  and  $G_{II}^c$ , hence  $\lambda$ . Equations (13) and (14) for the mode dependence of the parameters of the fatigue growth law are constructed following the same structure as (9) for the mode-dependent fracture toughness, which was suggested by Hutchinson and Suo (1992).

Next we shall discuss an interpretation of the previous equation, which allows a connection with a term frequently used in fatigue, that of damage accumulation at the tip. To this extent, Bolotin (1987) has offered damage accumulation arguments in discussing fatigue crack growth in connection with a mode-independent growth law. If we now assume that at specific mode mixity,  $\psi$ , the delamination needs  $N_i$  cycles of load to cause a jump of growth by  $\rho$ , then  $da/dN = \rho/N_i$ , and at the initiation of growth, the previous equation (12), gives:

$$1 - \bar{G}_{\max} = C(\psi)(\Delta \bar{G})^{m(\psi)} \frac{N_i}{\rho} = \int_0^{N_i} \frac{\partial \eta(N, \psi)}{\partial N} dN = \eta(N_i, \psi), \quad (15a)$$

where we have introduced the quantity  $\eta(N, \psi)$  that defines a measure of damage of the interlayer after  $N$  cycles at a prevailing mode mixity  $\psi$  (at a critical distance from the delamination tip). For undamaged material  $\eta = 0$ , and for fully damaged material (no resistance to growth)  $\eta = 1$ . Growth may take place at an intermediate value of  $\eta < 1$  if the interlayer resistance to growth has been reduced sufficiently as a result of the accumulated damage.

Now (15a) gives at the initiation of growth:

$$G_{\max} = \Gamma_0(\psi)(1 - \eta) = \Gamma_N(\psi). \quad (15b)$$

The above equation can be interpreted as the critical energy release rate,  $\Gamma_N$ , after  $N$  cycles at a prevailing mode mixity  $\psi$ . Notice that  $\Gamma_0$  is the mode-dependent critical energy release rate for the undamaged material. Naturally, the latter is reduced when damage is accumulated, in the linear manner specified by (15b). A more general, nonlinear variation would lead to a power on  $\bar{G}_{\max}$  in (12). In the interest of simplicity and since this would not affect the fatigue growth away from the fracture toughness region, a nonlinear variation was not adopted.

According to (15b), growth takes place when the critical energy release rate  $\Gamma_N$  is reduced to the level of the applied maximum energy release rate  $G_{\max}$ , i.e. if the accumulated damage becomes as shown in (15a). In fact, we have assumed that the damage accumulates with the number of cycles as:

$$\frac{\partial \eta(N, \psi)}{\partial N} = \begin{cases} 0 & \text{if } \Delta \bar{G} \leq (\Delta \bar{G})_{th}(\psi) \\ \frac{C(\psi)}{\rho} (\Delta \bar{G})^{m(\psi)} & \text{if } \Delta \bar{G} > (\Delta \bar{G})_{th}(\psi). \end{cases} \quad (15c)$$

Here  $(\Delta \bar{G})_{th}(\psi)$  is the threshold value of the energy release rate spread at a prevailing mode mixity  $\psi$ , which is required to cause damage, and  $m(\psi)$  and  $C(\psi)$  are material mode-dependent constants characterizing the resistance to the damage accumulation process and  $\rho$  is essentially a characteristic structural dimension (e.g. similar to the plastic zone size in metals) that may also be related to the layer thickness or interlayer spacing in the composite construction. To this extent, the complexity of identifying the precise relationship for a characteristic distance has already been pointed out in the study on the mode-dependent plastic zone size of interface cracks in glass-epoxy conducted by Liechti and Chai (1992). In that work, it was suggested that the inelastic behavior of the epoxy, frictional, and, perhaps, three-dimensional effects should be jointly considered in addition to other effects such as viscoelastic dissipation and interface asperity shielding.

Equation (12) is a semiempirical equation that describes the cyclic growth of delaminations. However, the previous arguments can be used to establish a rational base for this relationship by the hypothesis that, at the instant of growth, the delamination satisfies the Griffith equilibrium condition of the rate of total energy released (15b), where allowance has been made for the reduction in growth resistance of the material (critical  $G_c$ ) because of the previously accumulated damage near the delamination tip due to the cyclic loading-unloading.

Two loading parameters, the maximum value of the energy release rate near the tip of the delamination and the variation (spread) of this quantity in the loading-unloading cycle are taken to control the rate of delamination growth at a given level of mode mixity,  $\psi$ .

This hypothesis is validated in the next section by using it to correlate data from five configurations of delamination location through the thickness and at different applied maximum external compression. The results of this attempt at correlation of delamination extension rate data are discussed later. In spite of the wide range of combinations, the correlation will be shown to be very good. Hence, this formulation may be used to predict the number of cycles required to grow a delamination by a specific amount from simple laboratory tests of material properties and in conjunction with a reliable analysis for the near tip state of mode mixity and energy release rate. These laboratory tests would allow the measurement of the four constants of the fatigue law,  $\mu$ ,  $\kappa$ ,  $m_1$  and  $C_1$  and the two static fracture parameters,  $\lambda$  and  $G_I$ . They can be either the standard pure Mode I and pure Mode II tests discussed previously, or a set of static and cyclic delamination buckling, mixed mode tests that are correlated as presently shown.

### 3. DISCUSSION OF RESULTS

The theory described in the previous sections will now be applied to a specific configuration, consisting of a delaminated plate with  $E_1/(1-\nu_{12}\nu_{21}) = 151.6$  GPa

(typical of graphite-epoxy) and half-length  $L = 50.8$  mm. These dimensions correspond to our test specimen dimensions (a width of 12.7 mm has also been considered and is appropriately accounted for in the results). A delamination thickness of  $h = 0.4$  mm is assumed, whereas delamination length is varied. Furthermore, to ensure the same thin film model solution in the results that follow (for a chosen delamination length), we keep the delamination thickness constant and change only the plate thickness; this would give a varying ratio  $h/T$ . Concerning the toughness data, it was measured:  $G_I^* = 190 \text{ N m}^{-1}$  and  $\lambda = G_I^*/G_{II}^* = 0.30$ . These values are virtually identical to the values in Nilsson *et al.* (1993).

First, we need to determine the unstable-to-stable growth transition point,  $l_u$ , by examining the  $\bar{G}_{\max} - l$  curves (which would have zero slope or a peak value at this point); if the initial delamination length is below  $l_u$ , then unstable but contained growth will occur once the delamination grows to the length that corresponds to the critical energy release rate  $\Gamma_0$ . Figure 2(a) shows the maximum energy release rate  $\bar{G}_{\max}$ , as a function of the delamination length  $l/L$ , for a specified applied strain peak  $\epsilon_{\max} = 2.5 \times 10^{-3}$  and two cases:  $h/T = 0.10$  and  $h/T = 0.20$ , in comparison with the thin film solution. As has already been observed in Kardomateas and Pelegri (1994), the transition point is shifted to the left with respect to the corresponding point in the thin film solution. In each curve, two other points are of interest: the critical lengths,  $l_{cr1}$  and  $l_{cr2}$  on the rising and falling branches, respectively, at which  $\bar{G}_{\max} = 1$ .

In the growth law, it is assumed that the exponent ratio,  $\mu = m_{II}/m_I = 0.50$ , and the constant ratio,  $\kappa = C_{II}/C_I = 10$ . Moreover, the exponent  $m_I = 10$  and the constant  $C_I = 0.05 \text{ m cycle}^{-1}$ . These are typical values for graphite-epoxy. Let us now assume that the initial delamination half-length is  $l_0 = 25.4 \text{ mm} (= 0.5L)$ . From Fig. 2a, it is seen first that this delamination length corresponds to a point beyond  $l_u$  and beyond the critical length (at which  $\bar{G}_{\max} = 1$ ) in all three curves. Therefore, slow fatigue growth of the delamination is expected. Figure 2(b) shows the number of compressive cycles (between zero and  $\epsilon_{\max}$ ) that are needed to reach a corresponding delamination length on a semilogarithmic plot. It is seen that for the same actual delamination thickness, the lower  $h/T$  ratio (delamination closer to the surface) is more growth resistant than the higher  $h/T$  ratio (delamination located further inside the specimen). The thin film solution would predict a comparatively very fast delamination growth, i.e. a very poor cyclic growth resistance.

However, the thin film solution curve, which is the limit for a very low ratio of  $h/T$ , is not monotonic with respect to  $h/T$ . This is because the energy release rate vs applied strain curves tend toward the thin film solution for a decreasing ratio  $h/T$ , only in the beginning of the post-buckling phase, i.e. for relatively small applied strain (Kardomateas, 1993); as the applied strain is increased, the thin film model solution curve rises at a fast pace and predicts a much higher energy release rate.

Increasing the peak strain  $\epsilon_{\max}$  would produce some very interesting results. Figure 3(a) and (b) illustrates the behavior of the delamination for an initial delamination length  $l_0 = 15.24 \text{ mm} (= 0.3L)$  and  $\epsilon_{\max} = 3.6 \times 10^{-3}$ . This delamination length corresponds again to a point beyond the unstable-to-stable transition,  $l_u$ , and beyond the critical length, at which  $\bar{G}_{\max} = 1$  (Fig. 3a). Therefore, again, slow fatigue growth of the delamination is expected. Figure 3(b) gives the  $N - l$  curves on a linear plot (same growth law constants). The important observation is that the delamination

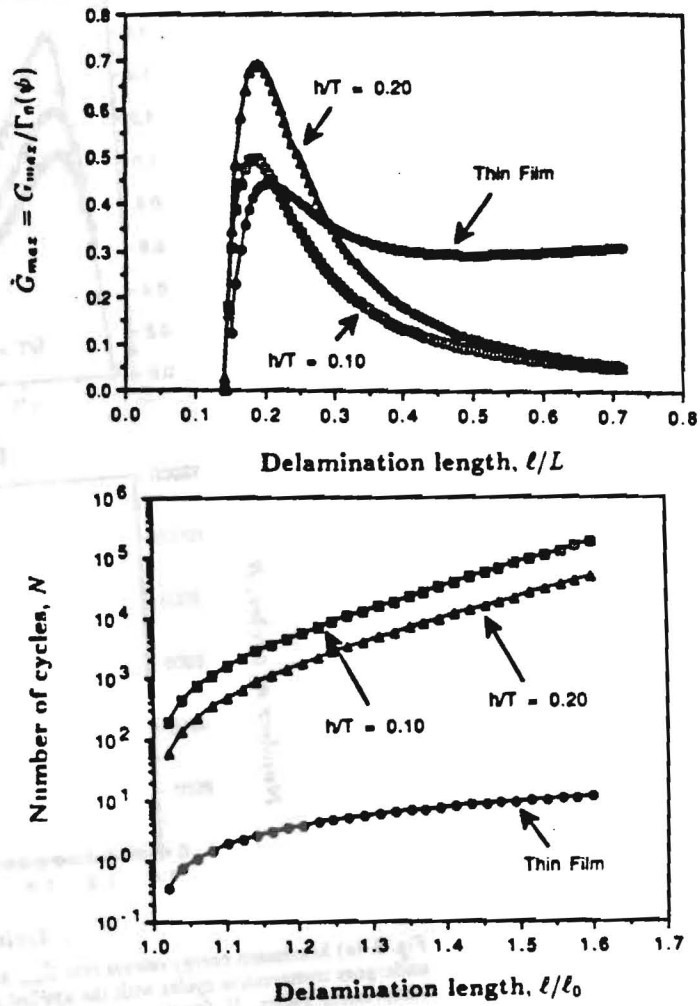


Fig. 2. (a) Maximum energy release rate  $\dot{G}_{max}$ , as a function of the delamination length. The configuration undergoes compressive cycles with the applied strain between zero and  $\epsilon_{max} = 2.5 \times 10^{-3}$ . (b) Number of compressive cycles,  $N$ , for a corresponding delamination length (semilogarithmic plot). An initial length  $l_0/L = 0.50$  has been assumed and  $\epsilon_{max} = 2.5 \times 10^{-3}$ .

would initially grow very rapidly (for  $h/T = 0.20$ , it would only take 230 cycles to reach a length of  $l = 30$  mm), and then it would grow very slowly. This would practically give the impression of an almost statically growing delamination followed by an arrest. This type of growth behavior was actually seen in the compression fatigue experiments that we performed on delaminated graphite-epoxy specimens with a relatively high  $h/T$  ratio. Specifically, in the 10/36 graphite-epoxy specimens (36 plies with the delamination between the 10th and 11th ply), it only took 870 cycles for the delamination to grow from 21.2 mm to 34.7 mm, i.e. by 63%, and then it needed 6,000 cycles to grow by an additional 19%, i.e. to 41.2 mm. Furthermore, for

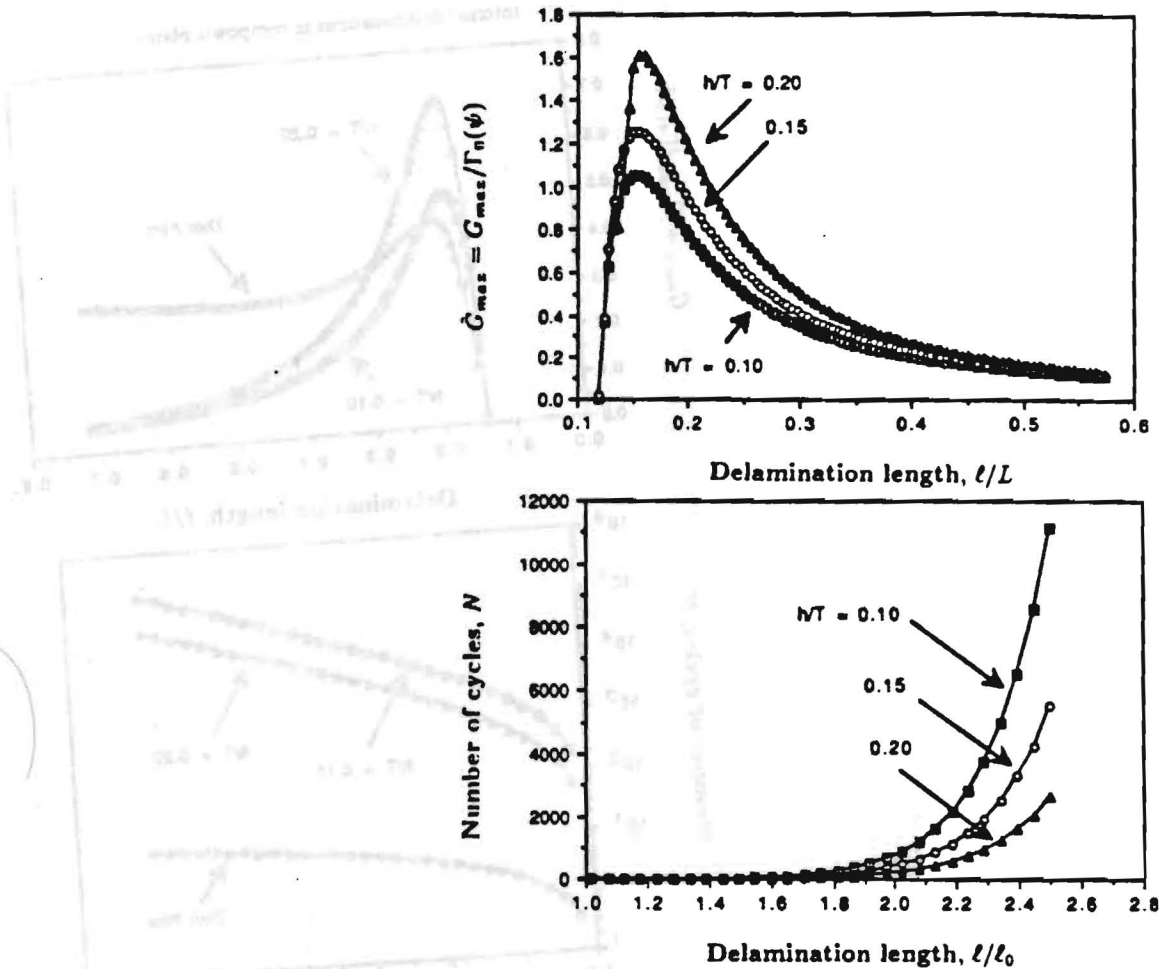


Fig. 3. (a) Maximum energy release rate  $\bar{G}_{max}$ , as a function of the delamination length. The configuration undergoes compressive cycles with the applied strain between zero and  $\epsilon_{max} = 3.6 \times 10^{-3}$ . (b) Number of compressive cycles,  $N$ , for a corresponding delamination length,  $l$ , on a linear plot. An initial length  $l_0/L = 0.30$  has been assumed and  $\epsilon_{max} = 3.6 \times 10^{-3}$ .

a delamination of a higher  $h/T$  ratio (located further inside the specimen), this initial fast growth interval is larger, i.e. the lower  $h/T$  ratio is again more growth resistant.

A comparison with results from cyclic compression experiments that were performed follows next. These experimental results are for a load ratio  $\alpha = 0$ . Before presenting and discussing them in detail, it should be pointed out that for an arbitrary load ratio  $\alpha$ , the following relationship can be proposed as a direct extension of (9).

$$\frac{da}{dN} = \frac{C(\psi)(\Delta\bar{G})^{m(\psi)}}{(1-\alpha) - \Delta\bar{G}} \quad (16)$$

Inclusion of the load ratio effects is hereby attempted in the same manner as in the

Forman *et al.* (1967) equation. The performance of this relationship, i.e. the load ratio effects, will be the subject of future investigations.

### 3.1. Experimental results

The experimental study was conducted on graphite-epoxy, procured from Amoco in the form of prepreg tape (commercial specification T50 6K ERL 1939-3) with about 33% of resin content and ply thickness of about 0.10 mm. Test panels were laid up by hand and cured in the Autoclave according to the manufacturer's recommended cure cycle, i.e. at a temperature of 350°F (177°C) and a pressure of 60 psi (a vacuum bag was placed prior to applying the curing cycle). The delaminations were introduced by placing at the desired location, through the width, a Dupont Teflon film of 0.025 mm (0.001 inch) thickness. Since the curing process affects the final dimensions of the specimens due to resin bleeding, the thicknesses of the specimens were measured after curing with a micrometer. The thickness measurements were taken at different points through the width and length to insure overall uniformity of the thickness and they were found to be satisfactory. The cured panels were carefully inspected for possible abnormalities, and were subsequently cut to specimen size using a silicon carbide blade.

The cyclic compression tests were conducted on these unidirectional graphite-epoxy specimens at a frequency of 1 Hz, and the delamination growth was monitored using a Questar remote video-measurement system. The experiments were at a constant  $\epsilon_{\max}$  and the property characteristics of the specimens are found to be as follows: modulus of elasticity  $E_1/(1 - \nu_{12}\nu_{21}) = 151.6$  GPa; critical energy release rates,  $G_i^c = 190$  N m<sup>-1</sup>,  $\lambda = G_i^c/G_{II}^c = 0.30$ ; exponent ratio,  $\mu = m_{II}/m_I = 0.501$ , constant ratio,  $\kappa = C_{II}/C_I = 10.01$ . These constants, which are typical of graphite-epoxy, were found from independent Mode I and Mode II tests. The specimens had a width  $w = 12.7$  mm and a half-length between the grips of  $L = 50.8$  mm.

Five delamination configurations were tested:

(a) 30 plies, specimen thickness  $T = 2.87$  mm, delamination of half-length  $l_0 = 21.25$  mm, between fourth and fifth ply, hence  $h/T = 4/30$ , and at a maximum compressive strain  $\epsilon_{\max} = 1.575 \times 10^{-3}$ . This specimen configuration is denoted as 4/30(A).

(b) 15 plies, specimen thickness  $T = 1.55$  mm, delamination of half-length  $l_0 = 25.86$  mm, between fourth and fifth ply, hence  $h/T = 4/15$ , and at a maximum compressive strain  $\epsilon_{\max} = 2.575 \times 10^{-3}$  (denoted as 4/15).

(c) 30 plies, specimen thickness  $T = 2.75$  mm, delamination of half-length  $l_0 = 26.15$  mm, between sixth and seventh ply, hence  $h/T = 6/30$  and at a maximum compressive strain  $\epsilon_{\max} = 1.325 \times 10^{-3}$  (denoted as 6/30).

(d) 30 plies, specimen thickness  $T = 2.87$  mm, delamination of half-length  $l_0 = 18.75$  mm, between fourth and fifth ply, hence  $h/T = 4/30$ , and at a maximum compressive strain  $\epsilon_{\max} = 1.247 \times 10^{-3}$ . This specimen configuration is denoted as 4/30(B).

(e) 36 plies, specimen thickness  $T = 3.00$  mm, delamination of half-length  $l_0 = 33.02$  mm, between tenth and eleventh ply, hence  $h/T = 10/36$  and at a maximum compressive strain  $\epsilon_{\max} = 1.003 \times 10^{-3}$  (denoted as 10/36).

These five test configurations exhibit different mode mixities and energy release rate spreads. Figure 4(a) shows the mode mixity,  $\psi$  as a function of the delamination

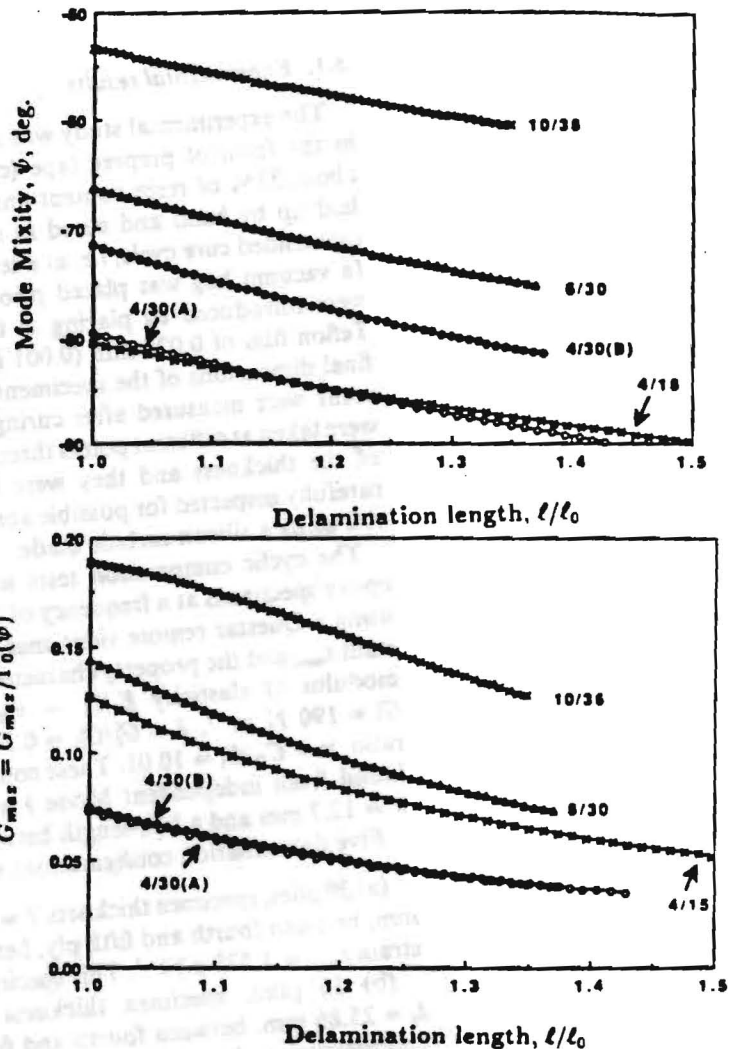


Fig. 4. (a) Mode mixity,  $\psi^0$ , vs delamination half-length,  $l/l_0$ , for the five specimen configurations tested ( $l_0$  is the initial delamination half-length). The pure Mode II is for  $\psi = \pm 90^\circ$ . (b) Maximum energy release rate  $\tilde{G}_{\max} = G_{\max}/\Gamma_0(\psi)$ , vs delamination half-length,  $l/l_0$ , for the five specimen configurations tested.

length, at  $\varepsilon_{\max}$ , for the five specimen configurations considered. It is seen that the 10/36 and 6/30 specimens exhibit the higher Mode I components. Figure 4(b) shows the energy release rate  $\tilde{G}_{\max} = G_{\max}/\Gamma_0(\psi)$  as a function of the delamination length, at  $\varepsilon_{\max}$ . All specimens are subjected to less than 20% of the critical energy release rate,  $\Gamma_0(\psi)$ , with the 10/36 and 6/30 specimens under a larger spread  $\Delta\tilde{G} = \tilde{G}_{\max}$ . Notice that the 4/30(A) and the 4/30(B) configurations have the same energy release rate  $\tilde{G}_{\max}$ , but distinctly different mode mixity,  $\psi$ .

Two data points, ( $l;N$ ), from the 4/30(A) specimen were used to obtain the constants  $m_1$  and  $C_1$ . These data points are: (30.48 mm; 231,354 cycles) and (30.734 mm; 253,155 cycles). The values obtained are:  $m_1 = 10.385$  and  $C_1 = 0.0435$  m/cycle.

Based on these values, Fig. 5(a) shows the actual experimental data and the predicted cycles for all five specimen configurations on a semilogarithmic plot. In all the experiments the delamination grew straight along the interface and the delamination length was measured with the help of a remote optical telescope/video-measurement system. It should be first emphasized that the same exponent and constant in the growth law are used for all delaminations, although each delamination configuration is characterized by a different location through the thickness, different initial length, different applied peak strain and different mode mixity. Since measurements were performed at discrete points, the measured data are given by discrete data points, whereas the predictions are represented by the lines. It is seen that the data form five distinct groups, each for each specimen type. First, an immediate observation can be made that the smaller the ratio  $h/T$  (delamination located closer to the surface), the slower the growth. Second, the experimental data seem to correlate adequately with the predicted values. For a more detailed record of the test data, Table 1 gives the

Table 1. Comparison with experiments, graphite-epoxy,  $G_I^* = 190 \text{ Nm}^{-1}$ ,  $\lambda = G_I^*/G_{II}^* = 0.30$ ; growth law,  $m_I = 10.385$  and  $C_I = 0.0435 \text{ m cycle}^{-1}$ ;  $\mu = m_{III}/m_I = 0.501$ ,  $\kappa = C_{III}/C_I = 10.01$

$h/T$ Specimen type	$l$ , mm delamination half-length	$N_{\text{theo}}$ Cycles predicted	$N_{\text{exp}}$ Cycles from tests
4/30(A) $l_0 = 21.25 \text{ mm}$ $T = 2.87 \text{ mm}$ $\epsilon_{\text{max}} = 1.575 \times 10^{-3}$	30.035	196,765	145,441
	30.658	246,705	244,825
	32.639	494,265	472,469
	32.753	513,915	539,485
4/15 $l_0 = 25.86 \text{ mm}$ $T = 1.55 \text{ mm}$ $\epsilon_{\text{max}} = 2.575 \times 10^{-3}$	35.623	4,488	6,107
	36.347	5,717	6,351
	39.522	15,521	14,413
	40.195	18,949	17,107
6/30 $l_0 = 26.15 \text{ mm}$ $T = 2.75 \text{ mm}$ $\epsilon_{\text{max}} = 1.325 \times 10^{-3}$	32.106	5,819	12,320
	33.668	9,869	12,795
	34.671	13,553	13,571
	35.801	19,075	14,065
4/30(B) $l_0 = 18.75 \text{ mm}$ $T = 2.87 \text{ mm}$ $\epsilon_{\text{max}} = 1.247 \times 10^{-3}$	23.635	87,244	65,307
	24.130	107,394	85,212
	24.841	143,019	138,718
	24.968	150,340	146,438
	25.781	205,410	236,154
10/36 $l_0 = 33.02 \text{ mm}$ $T = 3.00 \text{ mm}$ $\epsilon_{\text{max}} = 1.003 \times 10^{-3}$	34.671	584	320
	37.211	1,599	1,195
	38.100	2,028	1,612
	39.116	2,591	2,867
	40.132	3,251	3,671
	41.275	4,141	5,410

actual experimental data and the predicted cycles for all five specimen configurations. Figure 5(b) shows a picture of an actual 4/30(A) specimen undergoing cyclic compression at the point of peak compressive strain (buckled delamination, after growth by about 50%).

Of the five specimen configurations, the mode mixity is fairly similar between the 4/30(A) and 4/15 specimens, but distinctly different between the 4/30(A) and the 6/30 or 10/36 or 4/30(B) specimens [Fig. 4(a)]. In this context, in order to examine the importance of assuming a mode-dependent growth law, the predicted number of cycles for the corresponding mode-independent version of the growth law was calculated and compared to the experimental data. The following conclusions were made: if mode-independence was to be assumed in the growth law, which means that  $\mu = 1$  and  $\kappa = 1$ , then fitting the two constants,  $m$  and  $C$ , from the 4/30(A) data would fail to adequately predict the 6/30 data. Specifically, this would predict a number of cycles less than half those predicted by the present mode-dependent approach and the ones obtained from the experiments.

Finally, one additional observation should be made. For longer growth, i.e. beyond the point of the pure Mode II state, contact forces may be established, and this would have the effect of slowing the growth rate considerably. This was evident for the 4/30(A) specimen for growth beyond  $l = 33$  mm. The cycles needed for further advance for this type of specimen were about 1 million, as opposed to predictions of about 550,000. Since contact is not included in this formulation, these data points are not analyzed and are not part of the present paper.

#### 4. CONCLUSIONS

An experimental study of the fatigue growth of internal delaminations in composite plates which are subjected to cyclic compression was performed under constant strain amplitude and lead to the following conclusions:

(a) The delaminations would not grow in a static test; however, they do indeed grow after a sufficient number of buckling-unloading cycles

(b) The fatigue delamination growth is strongly affected by the relative location of the delamination through the plate thickness, the fatigue growth being slower for a smaller value of delamination thickness over plate thickness,  $h/T$ , (delaminations located closer to the surface).

(c) Delaminations located very near the surface, e.g.  $h/T = 2/30$ , did not grow even for a very large number of applied compressive cycles.

(d) The growth of the delaminations takes place under mixed-mode conditions characterized by a relatively high value of the Mode II component, which is increasing as the delaminations grow.

(e) A closed form analysis for the initial delamination post-buckling state, which does not impose any restrictive assumptions regarding the delamination thickness and plate length (as opposed to the usual thin film assumptions) is used in combination with a fracture mechanics treatment to obtain the energy release rate and the mode mixity at the delamination tip.

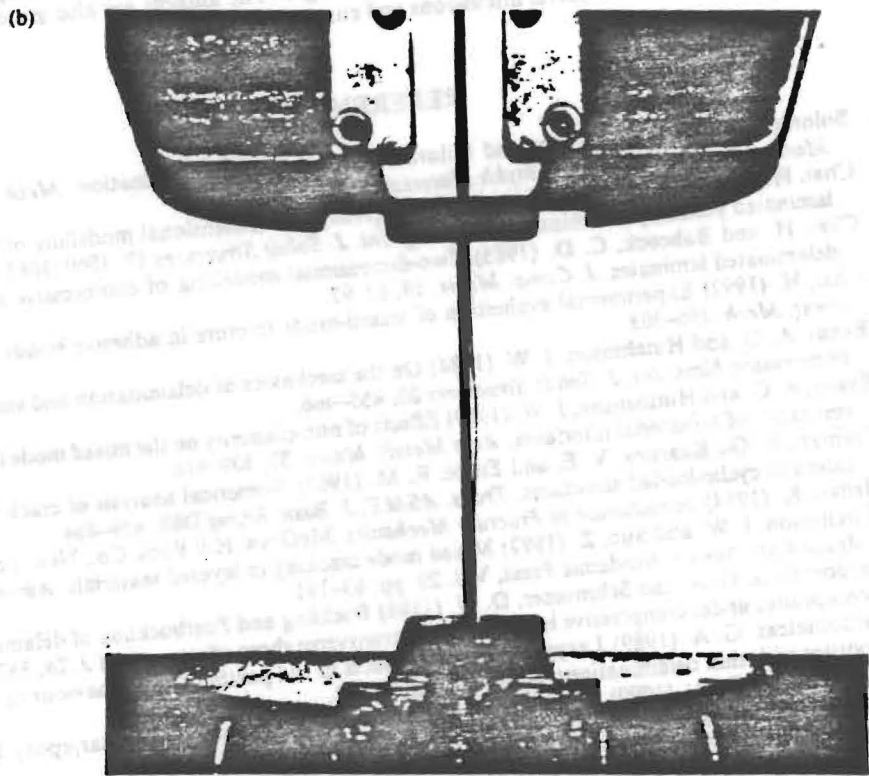
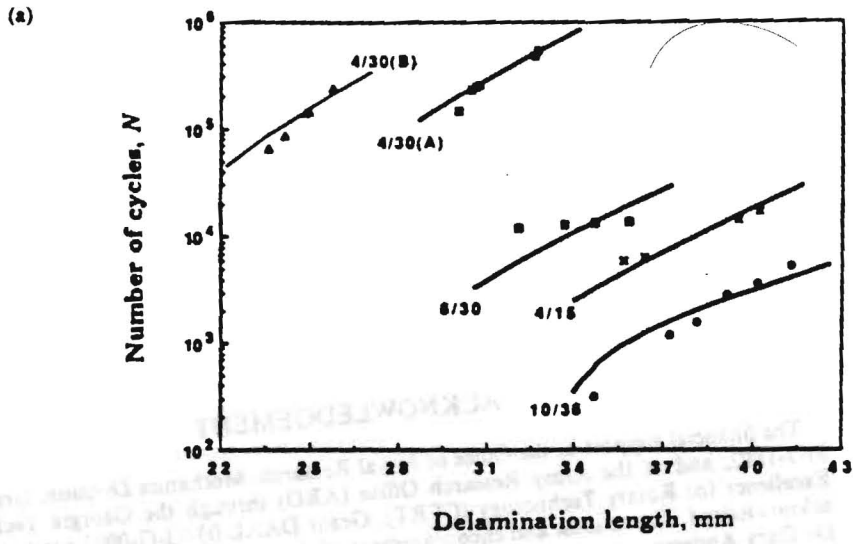


Fig. 5. (a) Fatigue delamination growth,  $N-l$  (semilogarithmic plot), for the five specimen configurations tested. In each case, the experimental data are denoted with discrete marks, whereas the lines represent the predictions of the theory. (b) An actual 4/30(A) specimen undergoing cyclic compression at the point of peak compressive strain (buckled delamination, after growth by about 50%).

(f) A mode-dependent cyclic growth law (12) is suggested, which is expressed in terms of the spread in the normalized energy release rate (10) in the pre- and post-buckling state, and in which the exponent and the constant are mode dependent (13, 14); it is shown to correlate well with the experiments, in spite of the different geometry (location of the delamination through the thickness, initial delamination length, plate thickness) and applied loading in each of the five delamination configurations tested. These tests were conducted on unidirectional graphite-epoxy specimens.

### ACKNOWLEDGEMENT

The financial support of the Office of Naval Research, Mechanics Division, Grant N00014-91-J-1892, and of the Army Research Office (ARO) through the Georgia Tech Center of Excellence for Rotary Technology (CERT), Grant DAAL 03-93-G-0002 are both gratefully acknowledged. The interest and encouragement of the Grant Monitors, Dr Y. Rajapakse and Dr Gary Anderson, are both gratefully acknowledged. The authors are also grateful to Professor R. L. Carlson for useful discussions and comments.

### REFERENCES

- Bolotin, V. V. (1987) Damage and failure of composites by delamination. *Mech. Compos. Mater. (Mekhanika Kompozitnykh Materialov)* 3, 424-432.
- Chai, H., Babcock, C. D. and Knauss, W. G. (1981) One dimensional modelling of failure in laminated plates by delamination buckling. *Int. J. Solids Structures* 17, 1069-1083.
- Chai, H. and Babcock, C. D. (1985) Two-dimensional modelling of compressive failure in delaminated laminates. *J. Comp. Mater.* 19, 67-97.
- Chai, H. (1992) Experimental evaluation of mixed-mode fracture in adhesive bonds. *Experiment. Mech.* 296-303.
- Evans, A. G. and Hutchinson, J. W. (1984) On the mechanics of delamination and spalling in compressed films. *Int. J. Solids Structures* 20, 455-466.
- Evans, A. G. and Hutchinson, J. W. (1989) Effects of non-planarity on the mixed mode fracture resistance of bimaterial interfaces. *Acta Metall. Mater.* 37, 909-916.
- Forman, R. G., Kearney, V. E. and Engle, R. M. (1967) Numerical analysis of crack propagation in cyclic-loaded structures. *Trans. ASME, J. Basic Engng* D89, 459-464.
- Hellan, K. (1984) *Introduction to Fracture Mechanics*. McGraw-Hill Book Co., New York.
- Hutchinson, J. W. and Suo, Z. (1992) Mixed mode cracking in layered materials. *Advances in Applied Mechanics*. Academic Press, Vol. 29, pp. 63-191.
- Kardomateas, G. A. and Schmueser, D. W. (1988) Buckling and Postbuckling of delaminated composites under compressive loads including transverse shear effects. *AIAA J.* 26, 337-343.
- Kardomateas, G. A. (1989) Large deformation effects in the postbuckling behaviour of composites with thin delaminations. *AIAA J.* 27, 624-631.
- Kardomateas, G. A. (1990) Postbuckling characteristics in delaminated kevlar/epoxy laminates: An experimental study. *J. Compos. Technol. Res. (ASTM)* 12, 85-90.
- Kardomateas, G. A. (1993) The initial postbuckling and growth behavior of internal delaminations in composite plates. *J. Appl. Mech. (ASME)* 60, 903-910.
- Kardomateas, G. A. and Pelegri, A. A. (1994) The stability of delamination growth in compressively loaded composite plates. *Int. J. Fracture* 65, 261-276.
- Kardomateas, G. A. and Pelegri, A. A. (1995) Growth behavior of internal delaminations in composite plates under compression: Effect of the end conditions. Submitted to the *Int. J. Fracture*.
- Kinloch, A. J. (1987) *Adhesion and Adhesives*. Chapman and Hall, London.

- Liechti, K. M. and Chai, Y. S. (1992) Asymmetric shielding in interfacial fracture under in-plane shear. *J. Appl. Mech. (ASME)* **59**, 295-304.
- Nilsson, K. F. and Storåkers, B. (1992) On interface crack growth in composite plates. *J. Appl. Mech. (ASME)* **59**, 530-538.
- Nilsson, K. F., Thesken, J. C., Sindelar, P., Giannakopoulos, A. E. and Storåkers, B. (1993) A theoretical and experimental investigation of buckling induced delamination growth. *J. Mech. Phys. Solids* **41**, 749-782.
- O'Brien, T. K. (1990) Towards a damage tolerance philosophy for composite materials and structures. *Composite Materials: Testing and Design (Ninth Volume)*. ASTM STP 1059 (ed. S. P. Garbo), pp. 7-33. American Society for Testing and Materials, Philadelphia.
- Russell, A. J. and Street, K. N. (1987) The effect of matrix toughness on delamination static and fatigue fracture under mode II shear loading of graphite fiber composites. *Toughened Composites*. ASTM STP 937, pp. 275-294. American Society for Testing and Materials, Philadelphia.
- Russell, A. J. and Street, K. N. (1988) A constant  $\Delta G$  test for measuring mode I interlaminar fatigue crack growth rates. *Composite Materials: Testing and Design (Eighth Conference)*. ASTM STP 972, pp. 259-277. American Society for Testing and Materials, Philadelphia.
- Sela, N. and Ishai, O. (1989) Interlaminar fracture toughness and toughening of laminated composite materials: a review. *Composites* **20**, 423-435.
- Sheinman, I. and Adan, M. (1987) The effect of shear deformation on post-buckling behavior of laminated beams. *J. Appl. Mech. (ASME)* **54**, 558-562.
- Simitses, G. J., Sallam, S. and Yin, W. L. (1985) Effect of delamination on axially loaded homogeneous laminated plates. *AIAA J.* **23**, 1437-1444.
- Storåkers, B. (1989) Nonlinear aspects of delamination in structural members. *Proceedings 17th International Congress of Theoretical and Applied Mechanics* (ed. P. Germain, M. Piau and D. Caillerie), pp. 315-336. North-Holland, Amsterdam.
- Suo, Z. and Hutchinson, J. W. (1990) Interface crack between two elastic layers. *Int. J. Fracture* **43**, 1-18.
- Wang, S. S., Zahlan, N. M. and Suemasu, H. (1985) Compressive stability of delaminated random short-fiber composites. Part I—Modeling and Methods of Analysis. *J. Comp. Mater.* **19**, 296-316.